Yehua TANG[1,2], Chunlan ZHOU[1], Wenjing WANG[1], Su ZHOU[1],
Yan ZHAO[1], Jianming FEI[1], Hongbin CAO[1]

Chinese Academy of Sciences (1), Graduate University of the Chinese Academy of Sciences (2)

EL and ITG Characterization of Large Areas Black Silicon Solar Cells VIA Screen Printing

Abstract. A simple process of texturing silicon (Si) surfaces using gold (Au)-catalyzed wet chemical etching was used to form black Si (BS) on a (100) p-type substrate. The surface became uniformly black after 6 min, with a resulting reflectivity of < 2% over the 400 nm to 1100 nm wavelength range. Large areas (153.18 cm^2) of black Si solar cells (BSSCs) with an n$^+$-p-p$^+$ structure were also fabricated using conventional processes, including POCl$_3$ diffusion, screen printing, and co-firing. The resulting cells were divided into two groups according to the emitter (46 and 37 $\Omega/\square$), and their output parameters were studied. The best convention efficiency (E$_{ff}$) was < 10%. The open-circuit voltage (V$_{oc}$) was particularly low because of poor surface passivation, and the shunt resistance (R$_{sh}$) linearly decreased with the series resistance (R$_s$). Electroluminescence (EL) and infrared thermography (ITG) measurements were conducted to characterize the BSSCs. Both the emissivity and temperature were low and non-uniform. Optimizing the fabrication process by reducing the etching depth and lowering the dopant sheet resistance led to significant improvement in V$_{oc}$ (~48 mV) and E$_{ff}$ (~3.8% absolute). EL and ITG measurements indicate that R$_s$ is another important factor that accounts for the poor properties of the BSSCs.

*Streszczenie. W artykule opisano proces teksturowania powierzchni krzemowej w procesie wytrawiania chemicznego z katalizatorem w formie złota, na potrzeby produkcji czarnego krzemu (BS) na podłożu p. Zastosowane rozwiązanie m. in. optymalizacji procesu teksturowania, poprzez redukcję głębokości wytrawiania dało znaczącą poprawę napięcia V$_{oc}$ oraz E$_{ff}$. Wykonane badania wskazują, że rezystancja szeregowa R$_s$ stanowi ważny czynnik wpływający na działanie ogniw słonecznych, zbudowanych z czarnego krzemu. (**Elektroluminescencyjna i termograficzna metoda charakteryzowania wielko-powierzchniowych ogniw słonecznych z czarnego krzemu – zastosowanie druku sitowego**).*

Keywords: Black Si solar cells, Au catalysis, EL measurement, ITG test.
Słowa kluczowe: ogniwa słoneczne z czarnego krzemu, katalizowanie złotem, pomiar elektroluminescencyjny, test ITG.

Introduction

Pyramid-shaped structures can be formed on silicon (Si) surfaces using a potassium hydroxide (KOH) solution. KOH is widely used in the Si solar cell manufacturing process to achieve a weighted reflectivity of approximately 13%. Reducing the surface reflectance is an effective method of obtaining high-efficiency cells. Hence, a simple process of preparing antireflective surfaces and integrating such surfaces into Si solar cells must be developed. Simulation results reported by Sai et al.[1] showed that the subwave structure (SWS), known as black silicon (BS), has a low mean reflectivity (below 3%) in a wide period range. They also demonstrated that an efficient reflection reduction can be achieved with the appropriate aspect ratio. Nishioka et al.[2] demonstrated that BS can be formed through simple wet chemical etching using a gold (Au) nanoparticle catalyst[3-6]. This technique can be applied to single and multicrystalline Si regardless of the orientation or doping type. When black silicon solar cells (BSSCs) were fabricated, a significant improvement (25% to 42%) in the short-circuit current (I$_{sc}$)[7, 8] was achieved with the antireflective BS structure.Other performance parameters, such as the open-circuit voltage (V$_{oc}$) and fill factor (FF), were not affected. In 2009, Yuan et al.[9] fabricated BSSCs on a 1 cm^2 floating zone (FZ) p-Si (100) substrate. The surface passivation layer was thermally deposited SiO$_2$, and the front electrode was prepared via photolithography and evaporation of Ti/Pd/Ag. A maximum efficiency (E$_{ff}$) of 16.8% was achieved without any antireflective coating. Photolithography, thermal oxidation, and evaporation are widely used at the laboratory scale to prepare high E$_{ff}$ Si solar cells, but they are not suitable for industrial application because of their high cost and complexity.

A fast and simple process of preparing large-area (153.18 cm^2) BS surfaces was developed using Au nanoparticle-catalyzed wet chemical etching in aqueous hydrogen fluoride (HF) and hydrogen peroxide (H$_2$O$_2$) at room temperature. The reflectivity over the 400 nm to 1100 nm wavelength range was < 2%. BSSCs with different dopant profiles were also fabricated via conventional

processes, such as phosphoryl chloride (POCl$_3$) diffusion, commercial paste screen-printing, and co-firing. Electroluminescence (EL) and infrared thermography (ITG) measurements showed that a lower sheet resistance is beneficial for cells. The V$_{oc}$ and FF of these cells were particularly low, and the best E$_{ff}$ was < 10%. Optimizing the fabrication process by reducing the etching depth and changing the dopant profile led to an E$_{ff}$ enhancement of ~3.8% (abs.) and a V$_{oc}$ enhancement of ~48 mV.

Materials and Methods

Samples were prepared from 180 μm thick, commercially available (100) p-type Czochralski (CZ) silicon wafers (~1.5 Ωcm, boron-doped). The samples were initially polished using HF and nitric acid (HNO$_3$) to remove the layer damaged by the saw wires. The samples were then thoroughly rinsed with deionized (DI) water. The samples were dipped into 0.4 mmol/L chloroauric acid (HAuCl$_3$) mixed with polyethyleneimine (PEI) for 2 min at room temperature to allow the deposition of the Au nanoparticle layer on the Si substrate. The initial PEI:HAuCl$_3$ molar ratio was 4:1. The samples were subsequently immersed in an etching solution of HF, hydrogen peroxide (H$_2$O$_2$), and DI water (HF:H$_2$O$_2$:H$_2$O = 1:5:10) at room temperature for 6 min. The etching mechanism was as follows: Si + H$_2$O$_2$ + 6HF → 2H$_2$O + H$_2$SiF$_6$ + H$_2$↑. The samples were then rinsed with DI water, and the residual Au nanoparticles were removed from the reaction mixture[2] by adding I$_2$:NH$_4$I:H$_2$O = 1:4:40 at 80 °C for 5 min. Finally, the samples were rinsed with DI water, blown dry with nitrogen, and subjected to further investigation. Reflectivity measurements were performed using a "Solar Cell Spectral Responser/QE/IPCE Measuement System" (Model: QEX 7) over the 300 nm to 1200 nm wavelength range.

BSSCs were fabricated in the production line. BS samples were initially immersed in chloroazotic acid at 80 °C for ~20 min to remove any Au residue prior to BSSC fabrication. After a standard RCA cleaning, the emitter diffusion was prepared in POCl$_3$ in a tube furnace. Two different emitters were used, namely, a high-ohmic emitter

with a mean sheet resistance ($R_\square$) of 46 $\Omega/\square$ and a low-ohmic emitter with $R_\square$ = 37 $\Omega/\square$. The latter was diffused through a reference cell, which was etched with aqueous KOH along the line (pyramid-structure surface). The $R_\square$ value was 46 $\Omega/\square$. After edge isolation and phosphosilicate glass removal, a SiNx layer (n=2.05, 80 nm), acting as an antireflection coating and passivation layer, was deposited via plasma-enhanced chemical vapor deposition. Both the rear and front metal contacts were fabricated using screen-printing commercial paste and through a co-firing process in an infrared conveyor belt furnace.

Results and Methods

Fig. 1. Reflectivity versus wavelength curve of etched black silicon (BS) surfaces at the different Au nanoparticle deposition times (ADT)

Table 1. Weighted reflectivity (R) of BS in random cones and pyramid samples at different ADTs.

Surface structure	ADT (min)	T (min)	Solution	R (%)
pyramid	-	28	KOH	13.60
random cones	2	6	HF,H_2O_2, H_2O	1.56
random cones	4	6	HF,H_2O_2, H_2O	1.45
random cones	6	6	HF,H_2O_2, H_2O	1.24
random cones	8	6	HF,H_2O_2, H_2O	1.26
random cones	10	6	HF,H_2O_2, H_2O	1.23

The reflectivity of the BS structures versus the wavelength at different Au deposition times (ADT) was investigated. Fig. 1 shows the reflectivity versus wavelength curves of all samples at different ADTs and at 6 min etching time. The weighted reflectivities (R) are summarized in Table 1, including that of a reference sample etched in a KOH solution at 80 °C for ~25 min. The reflection spectrum of the BS surface exhibited a typically low reflectivity (< 2%), particularly in the 400 nm to 1100 nm wavelength range. The morphology of the etched BS surface resembled random cones (data to be published elsewhere), and the width and depth were approximately 10 and 250 nm, respectively. Fig. 1 shows that the reflectivity varied with ADT, which may be due to the Au nanoparticle coverage rate. A longer deposition time allows a higher coverage rate and decreased surface reflectivity with increasing ADT.

Fig. 2 shows the illuminated output parameter (V_{oc}, I_{sc}, FF, and E_{ff}) distributions of the cells prepared on BS substrates with different dopant profiles. All parameters of the heavier dopant samples increased, especially V_{oc}. The best E_{ff} for the 46 $\Omega/\square$ samples was 8.39%, whereas that of the 37 $\Omega/\square$ samples was 9.43%. The average E_{ff} value of 50 reference cells was 17.2%. Detailed comparisons of the other electrical properties (including dark I-V and QE) of the BSSCs and the reference samples were also performed, and the results were published elsewhere. The R_{sh} versus R_s curves of all BSSCs (Fig. 3) clearly shows that R_{sh}

linearly decreased with R_s. This decrease may have been due to the high peak temperature during the firing process, or the BS structure itself. The BS layer is a nanoporous structure with a significantly increased superficial area, which allowed the easy etching of the Ag paste.
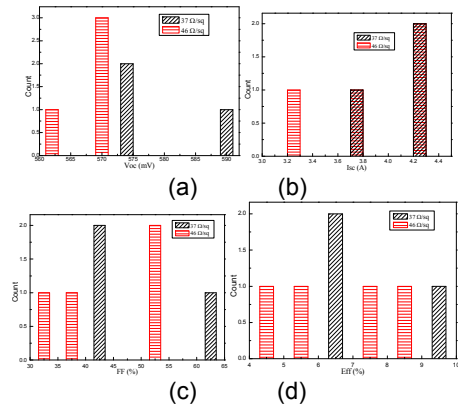

Fig. 2. BSSC output parameters showing the (a) open-circuit voltage, V_{oc}; (b) short-circuit current, I_{sc}; (c) fill factor, FF; and (d) efficiency, E_{ff} distributions
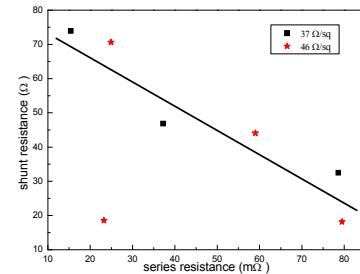

Fig. 3. R_{sh} versus R_s curve for the BSSCs

A forward current in the dark are shown in Fig. 4 The corresponding temperature distributions are shown in Fig. 5.
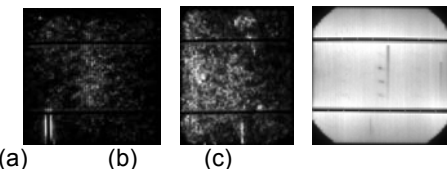

Fig. 4. Electroluminescence (EL) images of the emissivity distribution measured at a 5 A forward current: (a) 46, (b) 37, and (c) 46 $\Omega/\square$ reference cell
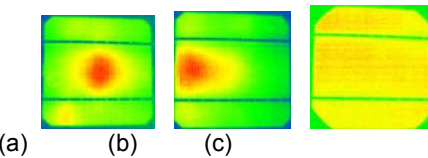

Fig. 5. Temperature distribution of the ITG images measured at a 5 A forward current: (a) 46 $\Omega/\square$ BSSC, (b) 37 $\Omega/\square$ BSSC, and (c) 46 $\Omega/\square$ reference cell

The reference cell exhibited a homogeneous emissivity (Fig. 4c), except for a few disconnected fingers and conveyors and a uniform temperature (Fig. 5c). The EL of the BSSCs was largely dark (Figs. 4a and 4b) and the temperature distribution was non-uniform compared with those of the reference. A careful comparison between Figs. 4a and 4b reveals an emissivity enhancement in the 37 $\Omega/\square$ cell. A heavier dopant (lower emitter sheet) enhances BSSC performance. In addition, a comparison between

Figs. 4 and 5 shows that the temperature was higher for the brighter areas in the EL image of the BSSCs. Hence, R_s was the dominant factor that caused the lower emission intensity of the BSSCs, indicating that the BSSCs benefited from the heavier dopant. The EL measurements for the BSSCs under a 12 V reverse bias in the dark were also performed, and the resulting images are all dark (data not shown). The BSSC output parameters are shown in Fig. 6. In general, the BSSC properties were significantly improved, especially V_{oc}. The 46 $\Omega/\square$ based cell samples etched for 4 min showed improved properties. The best E_{ff} for the samples etched for 4 min was 11.33%, and the Voc was 610 mV, compared with the 8.39% and 570 mV of the samples etched for 6 min, respectively. In the samples etched for 4 min, the 31 $\Omega/\square$ solar cells exhibited the best performance, with a maximum E_{ff} of 12.17% and a V_{oc} of 618 mV, indicating improved E_{ff} (~3.8% abs.) and V_{oc} (~47.9 mV). On the other hand, the Isc and FF of the 31 $\Omega/\square$ 4 min etched sample was 4.73 A and 64.5%, respectively, compared with the 4.37 A and 52.2% of the 6 min etched 46 $\Omega/\square$ samples. BS has a nanoporous structure that increases the superficial area and acts as a dead layer. The shortened etching time reduced the etching depth and surface recombination; hence, V_{oc} was significantly improved. V_{oc} remained lower than that of the reference cell (~620 mV) because of the poor surface passivation. Although Isc and FF were also affected by surface recombination, they slightly improved with the reduction in etching time, mainly because of R_s and R_{sh}. Gaps in the processing, which include the modification of the etching solution, the firing process, and related aspects, will form the bases of future studies.
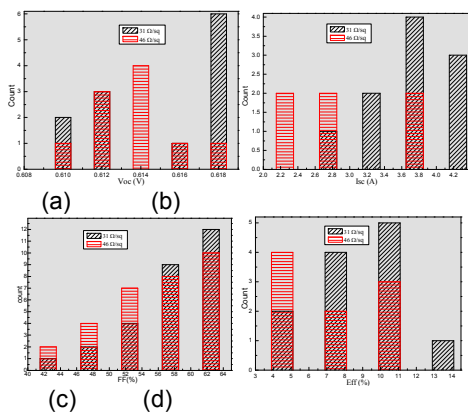

Fig. 6. Optimized BSSC output parameters showing the (a) V_{oc}, (b) Isc, (c) FF, and (d) E_{ff} distributions

Conclusion

Nanoporous subwave BS structures in random cones were formed via a wet chemical etching method catalyzed by Au nanoparticles. The reflectivity in the 400 nm to 1100 nm wavelength range was < 2%, and the BS exhibited favorable light-trapping properties. After etching the BSSC for 6 min, the resulting properties were much lower than those of the reference cell. EL and ITG measurements indicate that R_s was the main reason for this observation. Rsh linearly decreased with R_s. However, BSSCs can benefit from heavier doping emitters. Reducing the etching time to 4 min significantly improved the output properties. An improvement in V_{oc} (~48 mV) and E_{ff} (~3.8% abs.) was observed for the 31 $\Omega/\square$ solar cells compared to their 46 $\Omega/\square$ analogue. Other parameters also improved with shallower etching depths and lower dopant emitter contents. The output parameters and the EL and ITG measurements indicate that the properties of the optimized BSSCx were significantly improved.

REFERENCES
[1] H. Sai, H. Fujii, et al., Numerical analysis and demonstration of submicron antireflective textures for crystalline silicon solar cells, Photovoltaic Energy Conversion, Conference Record of the 2006 IEEE 4th World Conference on (2006), pp. 1191–1194.
[2] K. Nishioka, S. Horita, et al., Antireflection subwavelength structure of silicon surface formed by wet process using catalysis of single nano-sized gold particle, Solar Energy Materials and Solar Cells, vol. 92, (2008), pp. 919–922.
[3] S. Koynov, M. S. Brandt, et al., Metal-induced seeding of macropore arrays in silicon, Advanced Materials, vol. 18, (2006), pp. 633–+.
[4] T. K. Sarma, D. Chowdhury, et al., Synthesis of Au nanoparticle-conductive polyaniline composite using H2O2 as oxidising as well as reducing agent, Chemical Communications, (2002), pp. 1048–1049.
[5] K. Tsujino, M. Matsumura, et al., Texturization of multicrystalline silicon wafers by chemical treatment using metallic catalyst, 2003.
[6] K. Tsujino, M. Matsumura, et al., Texturization of multicrystalline silicon wafers for solar cells by chemical treatment using metallic catalyst, Solar Energy Materials and Solar Cells, vol. 90, (2006), pp. 100–110.
[7] S. Koynov, M. S.Btandt, et al., Black multi-crystalline silicon solar cells, PHYSICA STATUS SOLIDI-RAPID RESEARCH LETTERS, vol. 1, (2007), pp. R53–R55.
[8] K. Nishioka, T. Sueto, et al., Antireflection structure of silicon solar cells formed by wet process using catalysis of single nano-sized gold or silver particle, Photovoltaic Specialists Conference (PVSC), 2009 34th IEEE (2009), pp. 169–171.
[9] H.-C. Yuan, V. E.Yost, et al., Efficient black silicon solar cell with a density-graded nanoporous surface: Optical properties, performance limitations, and design rules, Applied Physics Letters, vol. 95, (2009), pp. 123501–123503.

Authors:*Yehua Tang,([1]Institute of Electrical Engineering, Key Laboratory of Solar Thermal Energy and Photovoltaic Systems, Chinese Academy of Sciences, Beijing 100190, P. R. China. [2]Graduate University of the Chinese Academy of Sciences, Beijing 100049, P. R. China),E-mail:tangyehua@mail.iee.ac.cn;*